Figure S1

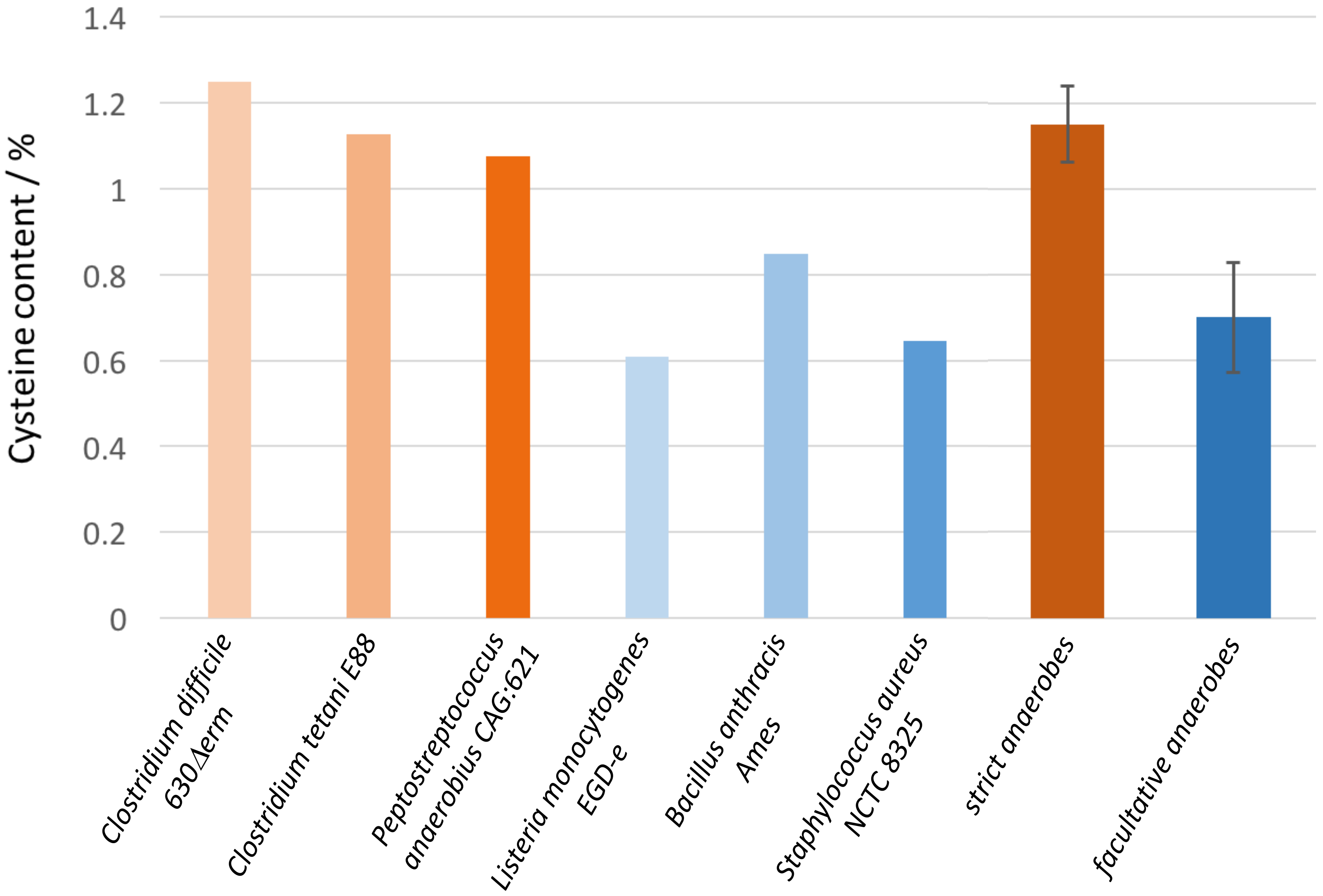

Fig. S1: Cysteine content of the proteomes of three strictly anaerobic pathogenic bacteria (brown color) and three facultative anaerobic pathogenic bacteria (blue). The three strict anaerobes exhibit a statistically higher content of cysteine than the three facultatively anaerobic bacteria.

Figure S2

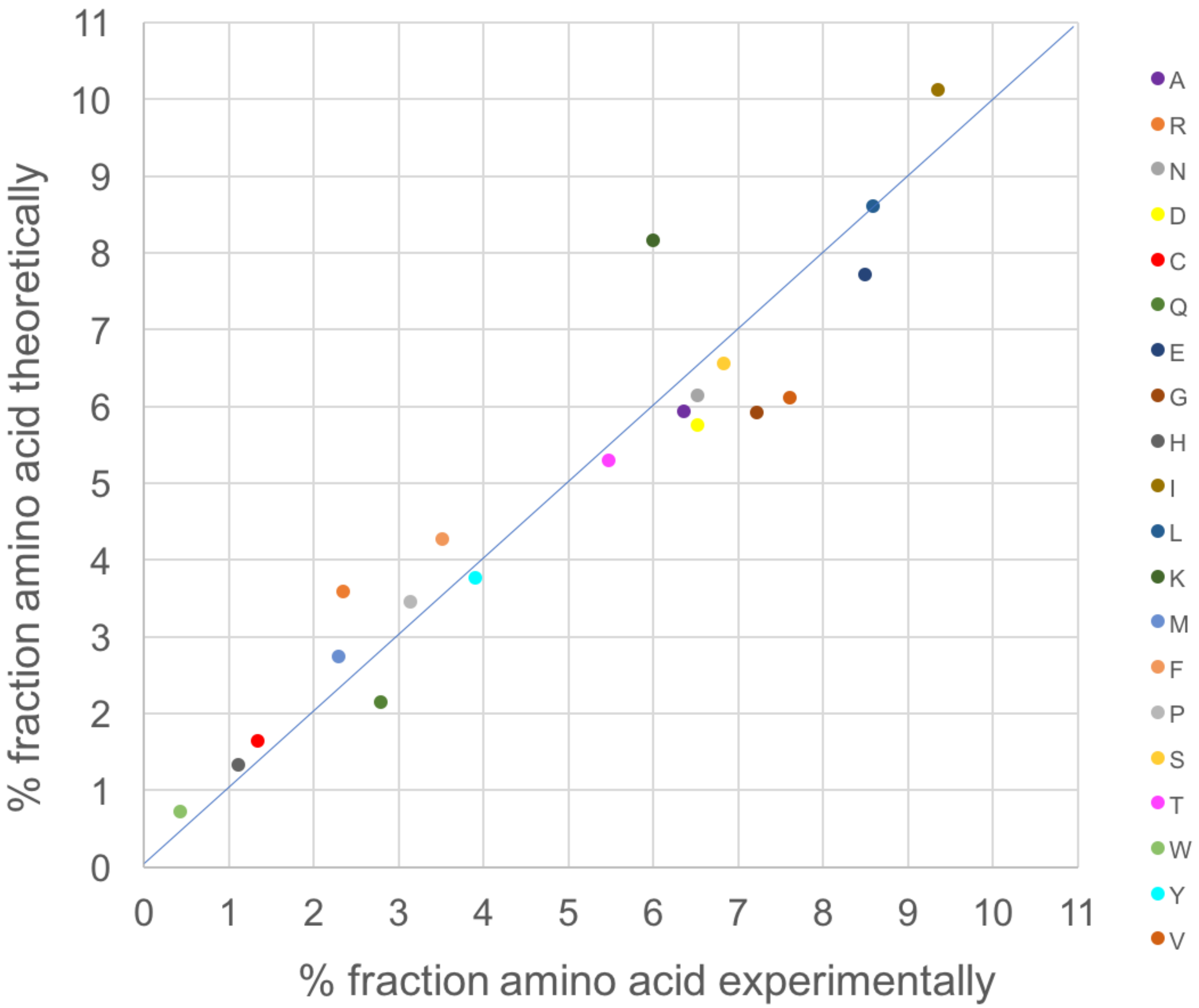

Fig. S2: Scatterplot of the percentaged fraction of amino acid residues experimentally identified and the percentaged fraction in the theoretical proteome of *C. difficile* for each of the 20 amino acids.

Figure S3

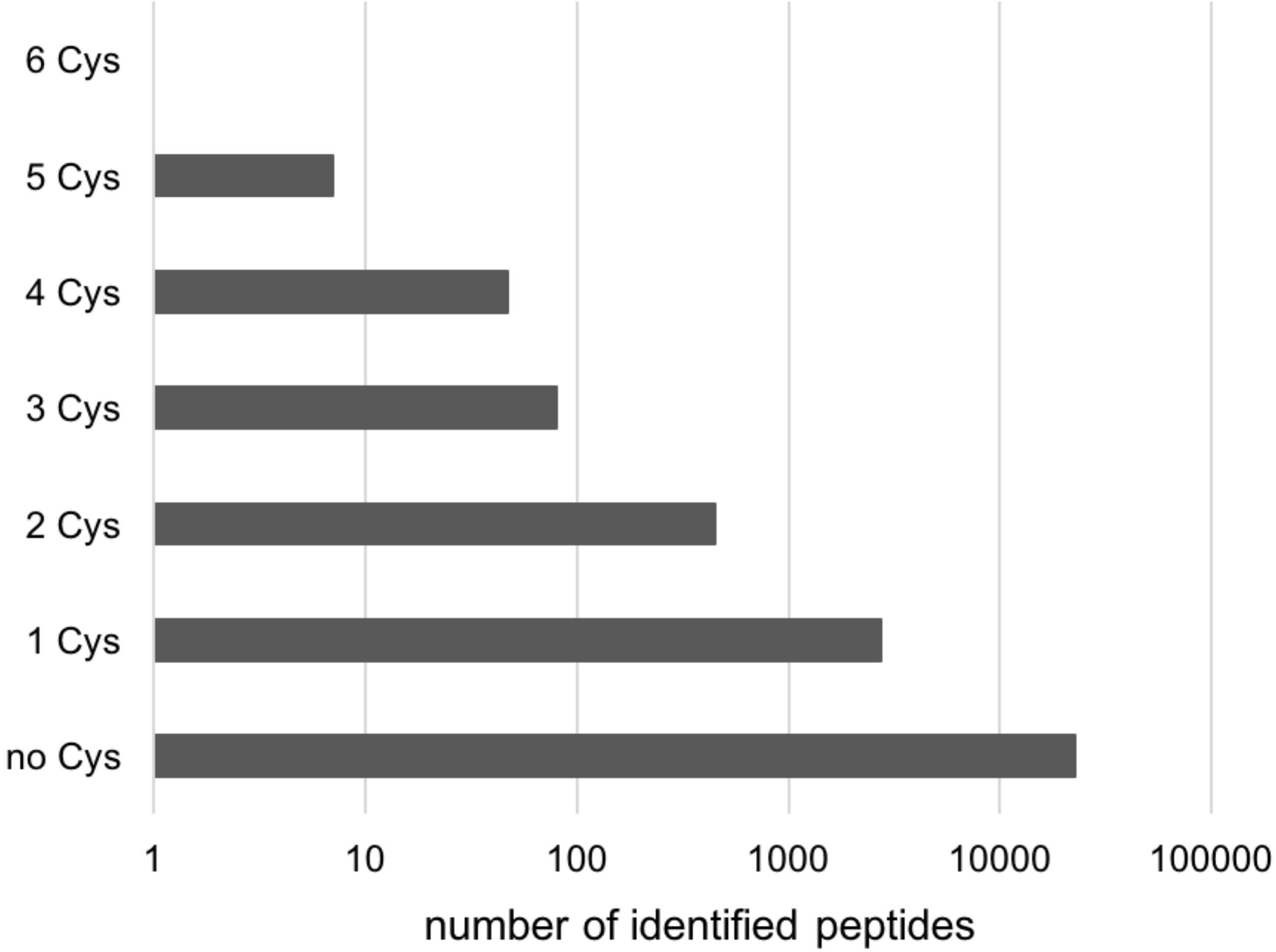

Fig. S3: Of the 26,380 detected unique peptides (different primary sequence) 3,332 peptides contain one or more cysteine residues. All cysteine containing peptide sequences are given supplementary in Table S1.

Figure S4

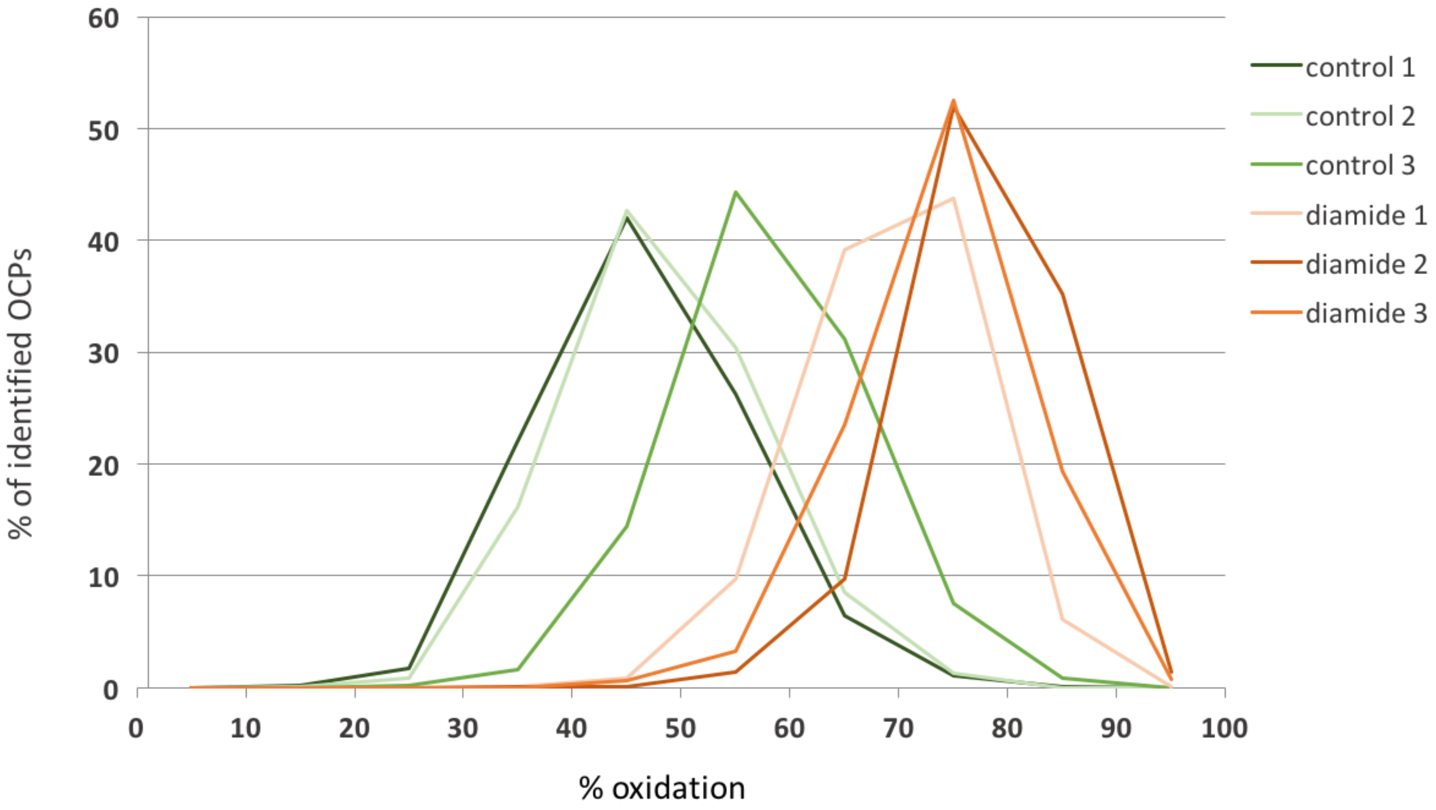

Fig. S4: Distribution of iodoTMT redox quantified OCPs according to their extent of oxidation. Three independent experiments of control samples and diamide shocked samples are plotted.

Figure S5

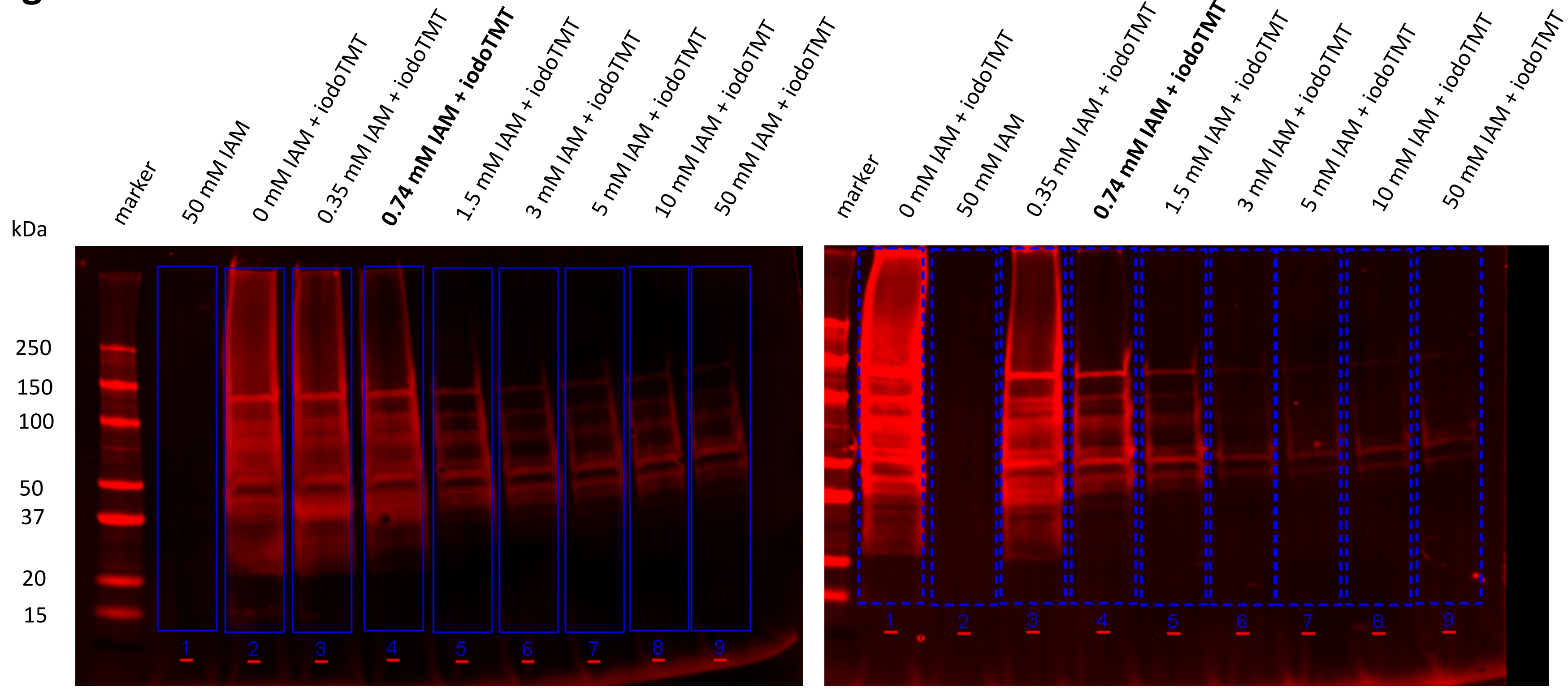

Name	Signal	Area	Bkgnd.
1	178	10414	4.60
2	64200	10414	4.78
3	49900	10414	4.72
4	32700	10414	4.61
5	11200	10414	4.48
6	6900	10414	4.43
7	6350	10414	4.37
8	6600	10414	4.34
9	4270	10414	4.49

Name	Signal	Area	Bkgnd.
1	70900	11094	6.61
2	-970	11094	6.24
3	44900	11094	6.23
4	15300	11094	6.13
5	6270	11094	6.00
6	1450	11094	5.99
7	1740	11094	5.93
8	1010	11094	5.93
9	1630	11094	5.94

Fig. S5: Proteins were alkylated in a 1st step with the specified concentrations of iodoacetamide (IAM) and in a 2nd step with iodoTMTzero. Proteins were separated by SDS-PAGE and iodoTMTzero detected via Western Blotting. A concentration of 0.74 mM alkylating agent in the 1st alkylation step corresponds to the amount used in the iodoTMT protocol for a differential cysteine labelling. Intensity of iodoTMT specific signals of the lanes is provided in the tables below. Results of two independent experiments are presented.

Figure S6

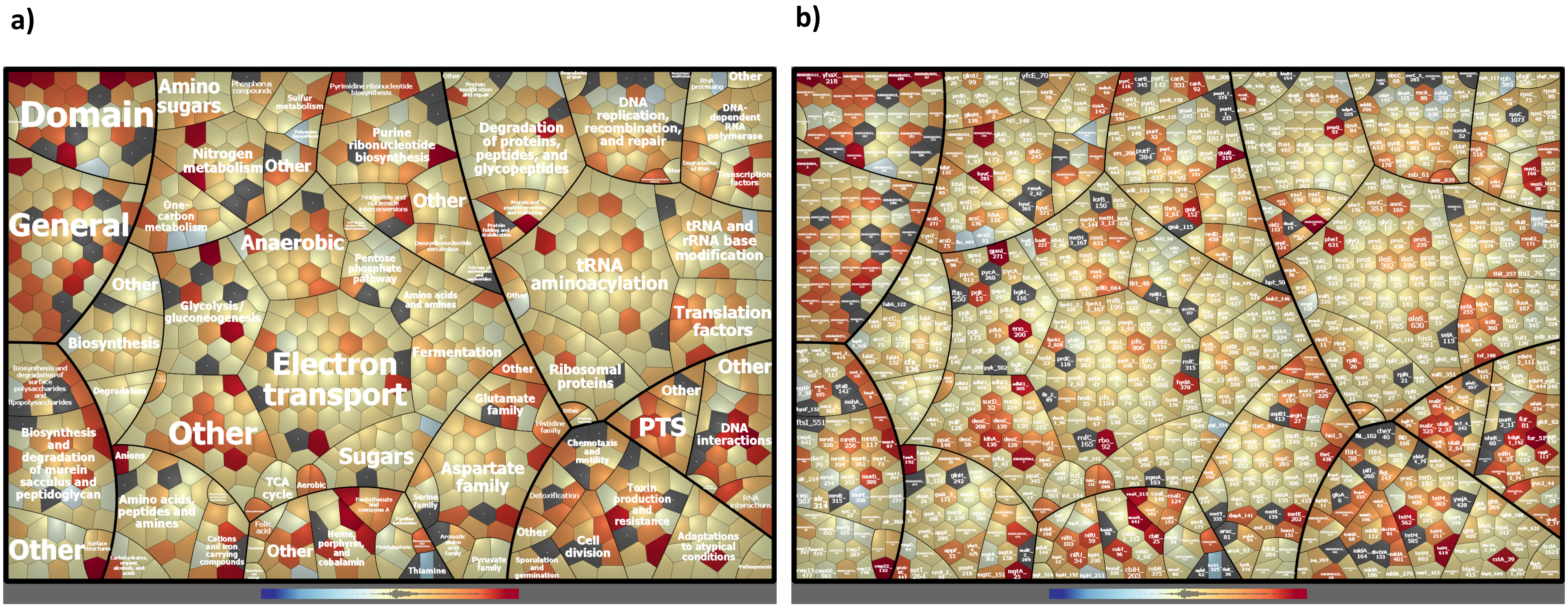
a)
b)
Domain
Amino sugars
Phosphorus compounds
Sulfur metabolism
Pyrimidine ribonucleotide biosynthesis
Purine ribonucleotide biosynthesis
Nitrogen metabolism
Other
Degradation of proteins, peptides, and glycopeptides
DNA replication, recombination, and repair
DNA-dependent RNA polymerase
RNA processing
Degradation of RNA
Transcription factors
General
One-carbon metabolism
Anaerobic
Pentose phosphate pathway
Nucleotide and nucleoside interconversions
2'-Deoxyribonucleotide metabolism
Protein and peptide secretion and trafficking
Protein folding and stabilization
tRNA aminoacylation
tRNA and rRNA base modification
Translation factors
Glycolysis/ gluconeogenesis
Amino acids and amines
Biosynthesis
Electron transport
Fermentation
Ribosomal proteins
Biosynthesis and degradation of surface polysaccharides and lipopolysaccharides
Degradation
Glutamate family
Histidine family
PTS
DNA interactions
Chemotaxis and motility
Biosynthesis and degradation of murein sacculus and peptidoglycan
Anions
Sugars
Aspartate family
TCA cycle
Aerobic
Amino acids, peptides and amines
Serine family
Pantothenate and coenzyme A
Detoxification
Toxin production and resistance
RNA interactions
Folic acid
Heme, porphyrin, and cobalamin
Aromatic amino acid family
Cations and iron carrying compounds
Carbohydrates, organic alcohols, and acids
Surface structures
Thiamine
Pyruvate family
Sporulation and germination
Cell division
Adaptations to atypical conditions
Pathogenesis

Figure S6

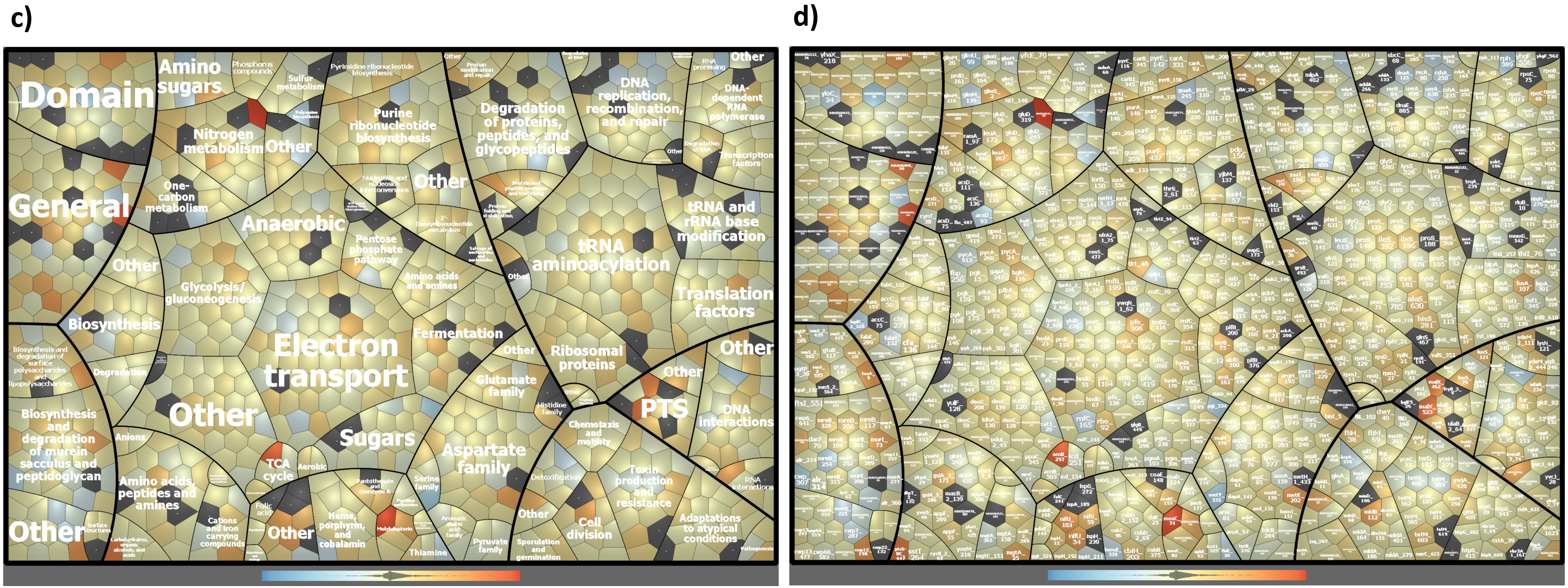

Fig. S6: Every cell in the Voronoi treemaps depicts the change in redox state of one of the 941 determined specific cysteine residues for the diamide *vs*. control experiment (a and b). Red colors represent oxidation, blue colors reduction and grey cells were not determined. Cells of the treemaps are arranged according to TIGRfam functional categories of the corresponding proteins with TIGRfam sub roles given in (a) and protein names and exact positions of cysteine residues in (b). Accordingly, results for the 929 cysteines of the bile acids *vs*. control experiment are depicted in (c) and (d).

Figure S7

a)

60% 6%

MSMLNKKTIEDIDV**C**GKKVLVR**C**DFNVPLQDGVITDENRLNGALPTIQYLISKGAK

-2%

VIL**C**SHLGKPKGEAKPELSLAPVAKRLSEMLGKEVVFAADDNVVGENAKKATEKME

5%

NGDVVLLENTRYRKEETKNEENFSKELASLAEIFVNDAFGTAHRAH**C**STVGAGEFL

4%

QERV**C**GYLIQKELKFLGEAVANPVRPFTAILGGAKVSDKLAVINELLEKVDNLIIGGG
MAYTFLKAQGYEVGTSLLEIDKVEYAKEMMEKAKNKGVNLLLPVDVVMADHFAP
DATPIVTEDANVKEDYMGLDMGPKTIANFVKTIKESKTVVWNGPMGVFEFENFA
NGTLSVARAMAELTDATTVIGGGDSAAAVNQLGFGDKMTHVSTGGGASLEFLEG
KELPGIAALDNK

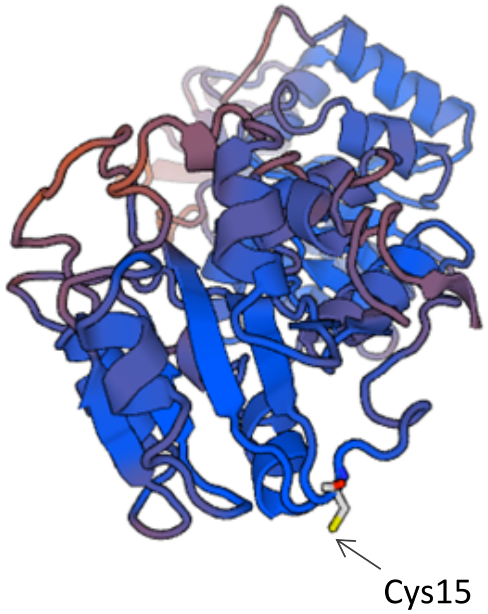

Fig. S7a: Phosphoglycerate kinase Pgk (A0A031WJX1) of *C. difficile* features five cysteine residues, which are enlarged and marked in red in the primary sequence. Underlined sequences of the protein have been identified. Percental increase in oxidation of redox-quantified cysteines after diamide shock is given on top of the according residues. All five cysteines of Pgk have been redox-quantified, but only Cys_{15} is significantly oxidized with an increase of 60%. According to the homologeous structure of 3-phosphoglycerate kinase of *Bacillus stearothermophilus* (SWISS MODEL id1php.1) Cys_{15} is surface exposed.

Figure S7

b)

MAFKMSTQKYSGKISEVEVGIGEKAIKLGGENVL
PFYSFDGEVGNSPKIGIQISDVYPESWTDSYKELYK

45% -16%
DVANCPVEWAKYVEANTQADFICLKFDGSDPNG

10%
LDKSVDECADVAKAVIEAIKLPLVVAGSGNHEKD

10%
GKLFEKLAQTLDGHNCLFMSAVEDNYKGVGASA
GMAYAHKVGAESSVDINLAKQLNVLLTQLGVKGE
NIVMNVGCSAVGYGYEYVASTMDRIRLAAFGQN

56%
DKTLQMPIITPVAFEVGHVKEAIAPIEDEPDWGC
PEERTIAMEVSTAASVLVGGSNAVILRHPKSIETIK
ELVNALA

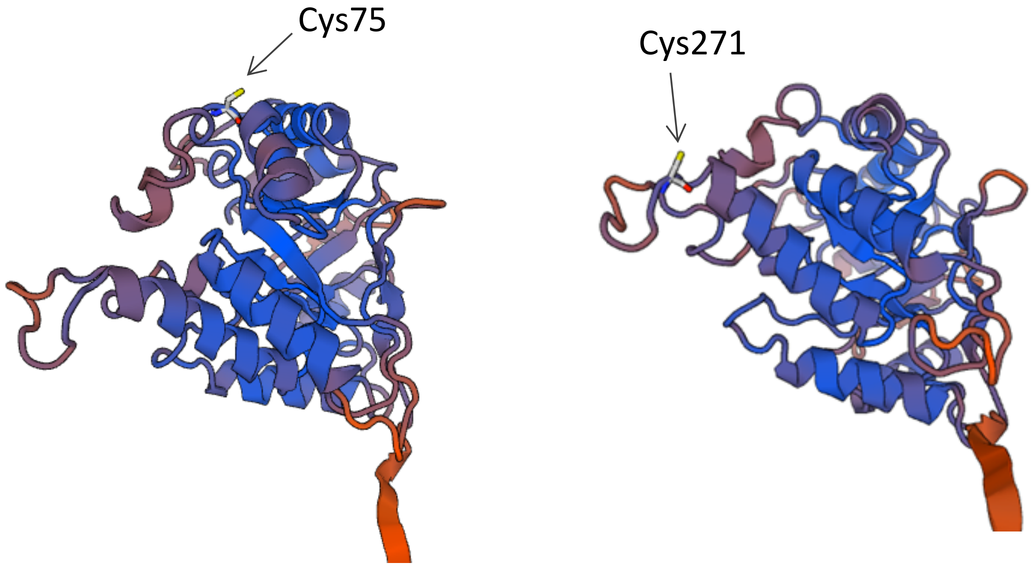

Fig. S7b: Five of six cysteines of Acetyl-CoA decarbonylase AcsD (A0A031WGJ0) could be redox-quantified. Two of them (Cys_{75} and Cys_{271}) were significantly oxidized by 45% and 56%, respectively. According to the homologeous structure of a folate-bound corrinoid iron-sulfur protein (id4dje.1) both cysteine residues are surface exposed.

Figure S7

c)

MSVGLDTVNNVESLVKKLAKIREAQKIFATYSQEQVDKIFLAASLAANKQRVPLAIMAQKETGMGIAEDK
9%
VIKNHYASEYIYNAYKETKTCGVIEKDEAFGMTKIAEPIGVIAAVVPTTNPTSTAIFKALLALKTRNGIIFSPH
PRAKNSTIEAAKVVLEAAVLAGAPEGIIGWIDEPSLELTTTVMKEVDLTLATGGPGMVKSAYSSGKPAIGV
GAGNTPAIIDDSADIKTAVNSILVSKTFDNGMICASEQSVIVLENIYNEVKKEFKERGAYLLDKDETEKIRNII
68%
LVNGGLNSKIVGQTACTIAKLAGFEVPVDTKVLIGEVESVEIEEAFAHEKLSPVLAMYKASDFDDAVRKAE
9%
KLVEDGGFGHTSSLYIDDVNQREKLDKFTSAMKTCRILINTPSSQGGIGDLYNFKLAPSLTLGCGSWGGN
4%
SVSENVGVKHLLNIKTVAERRENMLWFRAPEKVYFKKGCLGVALKELKDVMNKKRAFIVTDTFLYNNGY
6%
TKAVTDLLDEMNIKHTTFFEVEPDPTLECAKIGAKAMREFNPDVIISIGGGSAMDAGKIMWTLYEHPDV
DFQDLAMRFMDIRKRVYTFPKMGEKANFVAIPTSAGTGSEVTPFAVITDQDTGVKYPLADYELMPNMA
IVDSDMMMNMPKSLTSASGIDALTHALEAYVSMLATDYTNGLALQAIKSIFEYLPRAYDNGAKDPEARE
KMANASTMAGMAFANAFLGVCHSMAHKLGAFHHVPHGVANALLITEVMKFNSSDAPKKMGAFSQY
KYPEALKRYAGIASFLGLKGNSDEEKFQSLLVAIEDLKLKVGIPKSIKEFGVEESKFMDSIDEMVIQAFDDQ
2%
CTGANPRYPLMNEIKDMYLNSYYGR

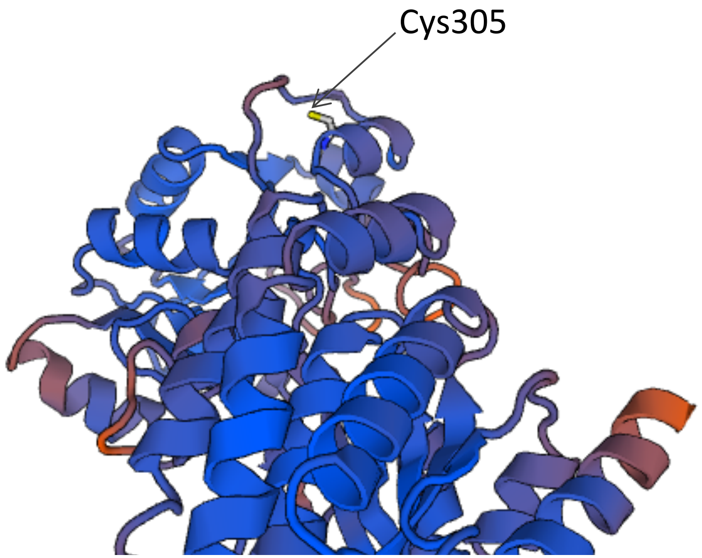

Fig. S7c: Alcohol dehydrogenase AdhE1 (A0A0A8U1W3) features nine cysteine residues. Six of them could be redox-quantified, but only Cys_{305} was significantly oxidized by 68%. In a homologeous structure of an acetylating aldehyde dehydrogenase from *Geobacillus thermoglucosidasius* (id5j78.1) Cys_{305} is located at the protein surface.